Communications
Research
Centre

LEVEL II ③

AD A093638

THEORY OF CONICAL-SCAN RADARS FOR
LOW-ANGLE TRACKING

by

J. Litva

DTIC
ELECTE
JAN 0 8 1981
E

DEPARTMENT OF COMMUNICATIONS
MINISTÈRE DES COMMUNICATIONS

CRC REPORT NO. 1336

DTIC FILE_COPY

CANADA

OTTAWA, 1980

81 1 06 004

COMMUNICATIONS RESEARCH CENTRE

DEPARTMENT OF COMMUNICATIONS
CANADA

THEORY OF CONICAL-SCAN RADARS FOR LOW-ANGLE TRACKING

by

J. Litva

(Radar and Communications Technology Branch)

CRC REPORT NO. 1336

August 1980

OTTAWA

CAUTION

The use of this information is permitted subject to recognition of proprietary and patent rights.

TABLE OF CONTENTS

THEORY OF CONICAL-SCAN RADARS FOR LOW-ANGLE TRACKING

by

J. Litva

ABSTRACT

In this report, a description of the tracking
behavior of conical-scan radars with low-angle
targets is presented. To begin, an equivalence
is established between monopulse and conical-scan
radars. Transformations are then developed from
this equivalence, which permit one to treat a
conical-scan radar as an equivalent monopulse
radar. An example is given of the use of these
transformations for simulating the low-angle
tracking behavior of conical-scan radars. The
simulated result is compared with a low-angle
conical-scan radar measurement. Since approxi-
mations are made in developing the theory
presented in this report, a discussion is given
on the range of tracking parameters for which
the theory is valid.

1. INTRODUCTION

In the first part of Section 1, the scope and purpose of this report
are presented. A brief introduction is then given, in the remainder of
Section 1, to the low-angle tracking problem and to monopulse and conical-
scan radars.

1.1 SCOPE AND PURPOSE

Theoretical results for describing the behavior of conical-scan radars
with low-angle targets are presented in this report. The theoretical
development takes advantage of the similarity in behavior of monopulse and

1

conical-scan radars. An equivalence will be demonstrated, which will allow us to formulate the problem of modelling conical-scan radars in terms of an equivalent monopulse radar. This approach is adopted simply because of the difficulty of developing a theoretical model of a conical-scan radar starting from basic principles.

In pursuing the equivalence approach, one effectively divides the main problem into two smaller problems. First, equivalent monopulse patterns are derived for the conical-scan radar. Secondly, one solves for the low-angle target signature of the conical-scan system using the existing monopulse radar theory (see Appendix A).

Simplifying assumptions are made in developing the monopulse equivalence relations. It will be shown that any errors resulting from these approximations will be small, or in other words, of second order.

A typical example of the use of the theoretical results developed in this report is presented in Section 6. The signature of a low-angle target tracked by a particular conical-scan radar is derived. The computed result is compared with a low-angle conical-scan radar measurement. Reasonable agreement will be seen to exist between these two results.

The primary purpose of this report is to demonstrate the equivalence between conical-scan and monopulse radars. Since conical-scan data are more readily available than monopulse data, the motivation for this work arises from a need for making results obtained by an analysis of these data accessible to furthering our understanding of the behavior of monopulse radars. A secondary purpose is to provide a better understanding of the behavior of conical-scan radars. The latter is an essential first step if the multipath performance of conical-scan radars is to be improved.

It is intended that in future work the material contained in this report be used to develop a theoretical model for conical-scan radars so that a parametric study can be made of their low-angle tracking performance. The model will permit use of existing experimental data for validating the conical-scan theory and ultimately help our gaining insights into monopulse radar theory. It is expected that the results given here will be used for improving the low-angle tracking behavior of monopulse radars. In fact, because of the equivalence established here, data and results obtained for and by either type of radar can in the future be used for improving the tracking performance of both.

1.2 THE LOW-ANGLE TRACKING PROBLEM

The accuracy of conventional tracking radars has been demonstrated to fall off quite markedly for targets over land and sea if the target's elevation angles are less than one or two beamwidths[1,2,3,4]. At these low elevation angles a portion of the electromagnetic (E-M) energy reflected from the surface of the sea or land is received by the radar. The interference of the direct and indirect E-M waves modifies both the amplitude and phase of the radar signals used for aligning the aperture of the radar with the incoming E-M waves (see Figure 1). This interference phenomenon, known as multipath interference, produces large errors in the measured target
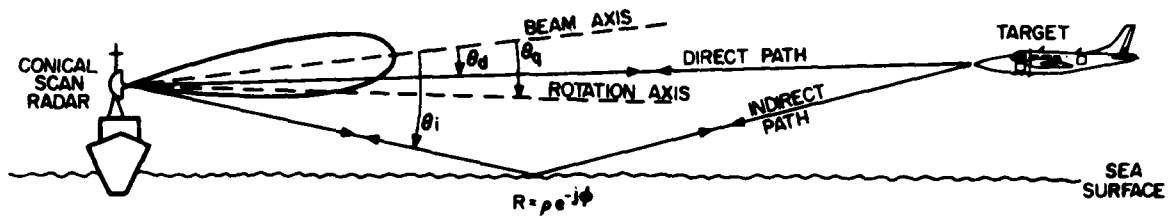
Figure 1. Low-angle Tracking Geometry for a Conical-scan Radar

elevation angle, whose magnitude usually approaches one beamwidth. Multipath interference can also cause a loss of track in the nulls of the radar's amplitude interference pattern. Although the problem has been known from the beginning of radar a solution has only been sought recently because of the growing threat to naval ships from very low flying anti-ship missiles - so called sea-skimmers.

1.3 TRACKING RADARS

Microwave tracking radars are used to measure coordinates of radar targets; usually, range, elevation and azimuth. Tracking radars used in association with weapons systems are normally called fire control radars. They are designed primarily to protect the vehicle in which they are located from air targets. Their measurements of target coordinates are used for fire control, or in other words, to predict future target positions, so that the carrier's weapons may be effectively deployed against targets. Shipborne and tank-based tracking radars usually operate at X-band. They are normally constrained to the higher end of the radar band of frequencies because of space and weight constraints imposed by the vehicles in which they are located. Long range ground-based systems, on the other hand, normally operate at S- or C-band to take advantage of lower radar wave propagation losses. In addition to tracking aircraft and missiles, ground-based systems are used for more exotic functions, such as tracking satellites.

The elevation and azimuth of a target are derived from measurements of the radar signal on two or more radar beams. These beams may be present at all times or may exist sequentially in time. It follows that the antenna terminal voltages will be different for the two beams, and if subtracted to form an error voltage, the result will be a function of the angle between the antenna boresight and the target's line-of-sight. The polarity of the error voltage specifies the polarity of the error angle. When the error voltage is zero, the antenna boresight coincides with the target's line-of-sight.

The method by which the squinted radar beams are formed defines the three generic types of tracking radars: Sequential lobing, conical-scan and monopulse (simultaneous lobing). Of the three types of tracking radars, the monopulse is the most recent in terms of technology and development. Conical scanned radars are the most common type found in active service. Sequential lobing radars represent a very old form of radar technology and are not likely to be encountered in practice. They were used primarily as target height finding radars.

1.4 MONOPULSE RADARS

Monopulse radars, as their name suggests, can measure the target's coordinates from a single radar pulse. They accomplish this by measuring the amplitude of the incoming signal on squinted overlapping beams that coexist continuously. The angle-of-arrival of the target can be derived from the ratio of the amplitudes of the signals received on the two beams.

In practice, the radar generates two new radar signals from the ones received by the squinted antenna beams. One is derived by summing the two signals and the other by subtracting the two signals. The resulting signals are called sum and difference signals. One can think of the sum and difference signals originating from sum and difference beams rather than from the elemental monopulse beams. The error signal is defined as the real part of the ratio of the difference signal and the sum signal (see Appendix A). Essentially, the error signal is the difference signal normalized by the sum signal so as to be independent of target cross-section and range. The sum signal is also used for target ranging and as a phase reference for defining the real part of the error voltage.

Since angle measurements are required in two dimensions, two error functions are required, one for azimuth tracking and the other for elevation tracking. Normally, monopulse radars have four beams which are divided into two pairs; one pair giving beams squinted along the vertical axis to measure elevation angle and the other pair giving beams squinted along the horizontal axis to measure azimuth angle.

Monopulse radars are capable of tracking single targets with an accuracy of 1-2 percent of the antenna beamwidth (BW). When tracking multiple targets separated by less than one BW, the radars' accuracy is degraded because of interference effects which produce erroneous error signals. A case in point is the low-angle tracking problem, where the target and its image are separated by less than one BW. For low-angle targets the accuracy of monopulse radars is reduced to 0.25-1.0 BW, depending on sea state. The greatest target tracking errors occur for perfectly smooth seas.

The behavior of monopulse radars tracking low-angle targets is quite well documented in the literature. White[5], for example, gives a low-angle target signature or plot of measured target height versus range for an experimental monopulse radar operating at S-band over smooth water. The S-band radar result shows a well-defined interference pattern. Whenever the change in range of the target resulted in the difference in path lengths for the direct and indirect signals to vary by one wavelength a cycle was added to the interference pattern. The peak-to-peak magnitude of the interference pattern is a function of the radar antenna BW and the angular separation of the target and its image. As the surface of the sea becomes perturbed a portion of the reflected or indirect signal, which previously was totally coherent, becomes random or diffuse and a noise-like component appears on the target signature. The ratio of the coherent to the incoherent components of the reflected signal decreases with increasing sea state. At about sea state 2-3, the target signature changes from being quasi-sinusoidal to becoming predominantly random or noise-like.

The theory for describing the behavior of monopulse radars with low-angle targets is also well documented in the literature[5,6,7,8]. White[5] derived a theory which agreed with experimental results. Equations for describing the low-angle behavior of monopulse radars are derived in Appendix A. Their development is very straightforward, which demonstrates the relative ease of modelling monopulse radars.

1.5 CONICAL-SCAN RADARS

Conical-scan radars[9] perform sequentially, by means of a rotating beam, what monopulse radars accomplish on a single pulse basis. The beam is offset with respect to the rotation axis by an angle called the squint angle. Typically, it is rotated about this axis at a rate of about 30 Hz. The rotating beam causes both the energy on target and the effective gain of the radar antenna to target echoes to be modulated (see Figure 2). These two effects impose a modulation on the radar signal. The amplitude of this modulation is a function of the magnitude of the target's error angle and its phase is a function of the elevation-azimuth components of the target's error angle. To remove the effects of changing radar cross-section and target range, the radar signal is normalized by the AGC of the radar receiver. The radar signal is then detected in an amplitude detector and low pass filter giving the radar error signal. Sine and cosine signals are generated by a two-phase generator which is driven by the mechanism that rotates the antenna beam. These signals are multiplied with the radar error voltage in product detectors and used for positioning the radar in azimuth and elevation (see Figure 3).
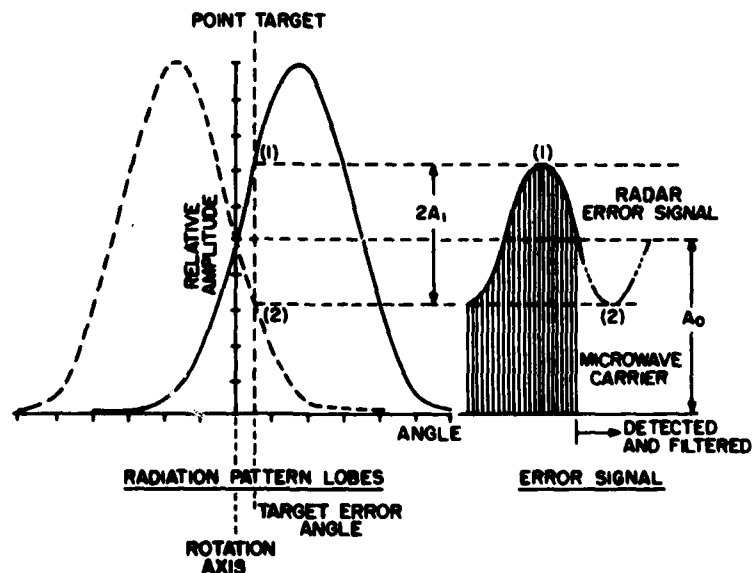

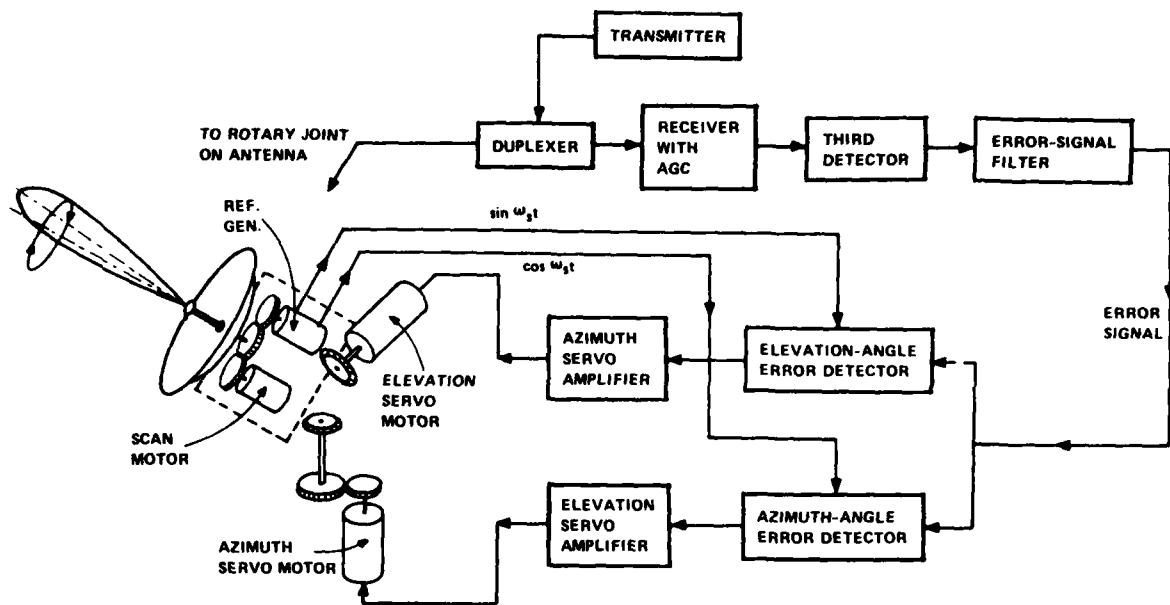Figure 2. Time Displaced Beam Pattern and Error Signal for a Conical Scan Radar (After: Damonti[12], et. al)

Figure 3. Block Diagram of Conical-scan Radar (After: Skolnik[9])

Very little work has been carried out to date on defining the behavior of conical-scan radars tracking low-angle targets. It is suspected that the reason for the absence of results is the expectation within the radar community of the eventual replacement of conical-scan radars by monopulse radars. Therefore workers have tended to concentrate on monopulse radars because they have the greatest probability of being chosen for any modifications which improve the performance of tracking radars. Even though it may be true that newly acquired tracking radars tend to be of the monopulse variety, it is also true that existing conical-scan radars are being refurbished so as to extend their operational life. This suggests a need for fully understanding the behavior of conical-scan radars; in particular, their behavior with low-angle targets.

Dax[8] stated that monopulse and conical-scan radars have similar low-angle tracking behaviors. An example of a low-angle result for a conical-scan radar operating at a frequency of 2.797 GHz is given by Dunn and Howard[10]. There is a close similarity between this result and that given by White[5] for a monopulse radar operating at a frequency of 2.857 GHz. An early conical-scan result is given by Fishback[11] which is consistent with those given by White and Dunn and Howard.

Barton and Ward[4] describe a procedure for constructing an equivalent difference pattern for a conical-scan radar. They suggest that a difference signal can be derived by subtracting the beam voltage patterns at the extreme positions of the radar's scan. The resulting pattern is found to consist of a split main lobe and sidelobes which are almost identical to the difference pattern of a monopulse system. They do not suggest a procedure for deriving an equivalent sum signal for a conical-scan radar.

A brief discussion of the equivalence of monopulse and conical-scan radars in given in Ref. 13. Some theoretical results are also presented.

Although the presentation is both hurried and sketchy, it was used initially as a guide in developing the theory presented in this report.

2. CONICAL-SCAN RADAR PARAMETERS

Conical-scan radar parameters are defined in the first part of Section 2. This is followed by a derivation for the error-voltage of a conical-scan radar tracking a low-angle target.

2.1 THE LOW-ANGLE GEOMETRY

The geometry for low-angle tracking with a conical-scan radar is given in Figure 1. There are two paths by which energy propagates from the radar to the target or from the target to the radar. These are the direct and indirect paths. The radar signals that propagate along these paths are called respectively the direct and indirect signals. At times it will be convenient to think of the indirect ray as originating from an image target. Although not shown in Figure 1, it is located directly below the target on the extension of the indirect ray from the radar to its point of reflection on the surface of the water. Whenever signals propagate along the indirect path, both their phase and amplitude are modified upon reflection from the surface of the water. The parameters defined* in Figure 1 are:

θ_q = radar squint angle (angle between the beam and rotation axes)

θ_d = angle of arrival of the direct ray with respect to the beam axis

θ_i = angle of arrival of the indirect ray with respect to the beam axis

R = complex reflection coefficient (ρ = magnitude of reflection coefficient; ϕ = phase of reflection coefficient).

2.2 CONICAL-SCAN RADAR RF VOLTAGE

By referring to Figure 1, one can write the magnitude of the direct signal at the target as

$$G'(\theta_d)E_o e^{j\omega t} \tag{1}$$

where ω = angular frequency of transmitter, radians/sec

$G'(\theta)$ = antenna voltage gain.

---

* *These are shown here at a particular instant when the beam axis, rotation axis, direct path and indirect path happen to lie in the same plane. A more general situation is given in Figure 4.*

8

The parameter E_o in eqn. (1) is given by

$$E_o = \frac{1}{r}\left(\frac{\eta P}{4\pi}\right)^{\frac{1}{2}} \tag{2}$$

and gives the amplitude of the electric field at the target for a radar antenna which radiates isotropically in free space,

where r = range to the target

            P = peak power

            η = impedance of free space (η = E/H)

Similarly, the magnitude of the indirect signal at the target is given by

$$G'(\theta_i)\rho\, E_o\, e^{j(\omega t - \Phi)} \tag{3}$$

where Φ = the total phase difference with respect to the direct path, due to both reflection and path length difference.

            ρ = the magnitude of the reflection coefficient.

The total RF electric field, E_{TT} at the target is

$$E_{TT} = G'(\theta_d)E_o\, e^{j\omega t} + G'(\theta_i)E_o\rho\, e^{j(\omega t - \Phi)} \tag{4}$$

Let us now trace the radar signals back to the radar by both the direct and the indirect paths.

The radar RF voltage, due to the direct signal, is proportional to

$$G'(\theta_d)E_{TT}, \tag{5}$$

and that due to the indirect signal is proportional to

$$G'(\theta_i)\rho\, e^{-j\Phi}\, E_{TT}. \tag{6}$$

The total radar RF voltage V_T^C is proportional to

$$G'(\theta_d)E_{TT} + G'(\theta_i)\rho\, E_{TT}\, e^{-j\Phi}. \tag{7}$$

and can be written in the form

$$V_T^C = K\, E_o\left\{G(\theta_d)e^{j\omega t} + 2G'(\theta_i)G'(\theta_d)\rho\, e^{j(\omega t - \Phi)} + G(\theta_i)\rho^2\, e^{j(\omega t - 2\Phi)}\right\} \tag{8}$$

where $\quad G(\theta)$ = antenna power gain = $[G'(\theta)]^2$

$\quad\quad K$ = parameter, which is a function of target range*, target cross-section and radar wavelength.

If we define the real part of $[V_T^C]$ to be V_T, then

$$V_T = K\ E_o\{L\ \cos\omega t + M\ \cos(\omega t-\Phi) + N\ \cos\ (\omega t-2\Phi)\} \quad\quad (9)$$

where

$$L = G(\theta_d), \quad\quad\quad\quad (10)$$

$$M = 2\rho G'(\theta_i)G'(\theta_d), \quad\quad\quad\quad (11)$$

and

$$N = \rho^2 G(\theta_i). \quad\quad\quad\quad (12)$$

Expression (9) gives the RF radar voltage for a conical scan radar tracking a low-angle target over a perfectly smooth sea surface. The first term describes the signal that propagates out to the target and back again, totally by the direct path. The second describes two signals; one that propagates out to the target via the direct path and back again via the indirect path and another that propagates along these same two paths but in the reverse direction. The last term accounts for the effect of the signal that propagates out and back again via the indirect path.

A deeper appreciation for the basic principle underlying conical-scan radars can be obtained from Figure 2. This figure shows the antenna beam intercepting a target at two different instances separated by one-half of an antenna scan period. Taken together these two beam patterns are defined to be the time-displaced conical-scan beam pattern. As the antenna beam rotates, its point of intersection with the target axis moves from point (1) to point (2) and back again. This motion causes the radar signal [eqn. (9)] to become modulated by signals having frequency f_s and harmonics of f_s, where f_s is the antenna rotation rate.

For a single target the amplitude of the modulation A_1 is proportional to the offset of the target line-of-sight with the antenna rotation axis. The radar error signal is normalized by the dc component of the radar signal. A_0 is used as an AGC signal for controlling the gain of the radar receiver's IF amplifiers.

2.3 DEFINITION OF ANTENNA BEAMS

The antenna voltage gain G' in eqn. (8) can be represented by a number of functions, such as, $\sin x/x$, $\cos^2 x$, e^{-x^2}, etc.. Skolnik[9] [p. 171, eqn.

---

* _It has been implicitly assumed that for purposes of deriving the magnitude of the target echo the direct and indirect path lengths can be taken to be equal._

5.2], for example, uses a Gaussian function, which when expressed as a voltage gain can be written as

$$G'(\theta) = G_o^{\frac{1}{2}} e^{-\frac{a^2}{2} \theta^2} \qquad (13)$$

where
θ = angle in degrees between the antenna-beam axis and the target axis

G_o = maximum antenna power gain

a^2 = constant = $2.776/\theta_B^2$ where θ_B is the 3 dB beamwidth measured in degrees.

Two functional representations will be used in this report for defining radar antenna beam patterns. One is based on the Gaussian function and the other on a composite of sinx/x functions. They both give patterns which are representative of typical fire control radar beam patterns, but with varying degrees of accuracy. The first tends to be less accurate than the second, mainly because it underestimates the magnitude of the antenna sidelobes. On the other hand the computational complexities inherent in its implementation are less than with the second. In terms of meeting the main objective of this report, to demonstrate the equivalence of monopulse and radars, they will be seen to give similar results.

3. ANTENNA SCANNING FUNCTION

We will find that to treat conical scan radars theoretically one needs to define an antenna scanning function.

3.1 DEFINITION

As a result of its rotation, the gain of a conical-scan beam along a target axis is a function of time, if the rotation and target axes are not coincident. The antenna gain along the target axis can be expressed in terms of a series similar to a Fourier series. This series has been called the antenna scanning function in the NATO Sub Group 4 Report[13]. We will follow this nomenclature here.

The form of the antenna scanning function is rather important because it is used for deriving the radar error signal. With the radar error signal one is able to deduce the characteristics of conical-scan radars with low-angle targets.

In Figure 3 are illustrated the processes that take place within a conical-scan radar in deriving an error signal. These are described in greater detail in Section 4.2. Basically, the antenna scanning function is used to describe the first step in this derivation, that is, reception of the direct and indirect rays with a rotating beam.

3.2 ANTENNA SCANNING FUNCTION FOR GAUSSIAN ANTENNA BEAMS

Skolnik[9] derived an antenna scanning function for the Gaussian antenna beam given by eqn. (13). His notation differs from that used here. Skolnik called his function the "antenna scan-modulation factor". Because of its importance, Skolnik's derivation is repeated here.

Consider Figure 4, which gives a head-on view of a conical-scan antenna beam. Angles θ_q, θ and θ_T are defined in this diagram by lengths of arc $\mu\theta$, $\mu\theta_q$, $\mu\theta_T$ on a sphere of radius μ. A somewhat restricted definition of the first two was given earlier in the discussion of Figure 1. Here we see that θ represents either θ_d or θ_i, depending on whether the target or its image is under consideration, θ_q defines the angle between the antenna beam and rotation axes and θ_T the angle between the antenna rotation and target axes. The angle ξ_s defines the rotational phase of the antenna beam with respect to a reference axis; ξ_0 is the angle defined by the target and the reference axis. Since the distance $\mu\theta$, $\mu\theta_q$, and $\mu\theta_T$ are small, they may be related by the law of cosines to the angle $\xi_s-\xi_0$

$$(\mu\theta)^2 = (\mu\theta_q)^2 + (\mu\theta_T)^2 - 2\mu^2\theta_q\theta_T \cos(\xi_s-\xi_0). \tag{14}$$

The substitution of θ into eqn. (13) from eqn. (14), with $G_0=1$ gives the antenna scanning function

$$G'(\theta) = \exp[-a^2(\theta_q^2 + \theta_T^2)/2] \, \exp[a^2\theta_q\theta_T \cos(\xi_s-\xi_0)]. \tag{15}$$

In this report we call eqn. (15) the Skolnik antenna scanning function. The following realtionship may be derived from expressions for Bessel functions

$$\exp(x \cos\psi) = I_0(x) + 2 \sum_{n=1}^{\infty} I_n(x)\cos n\psi, \tag{16}$$

where $I_n(x)$ is the nth-order Bessel function of imaginary coefficient. [Skolnik erroneously used $\exp(-x \cos\psi)$.] In Whittaker and Watson[14], $I_n(x)$ is
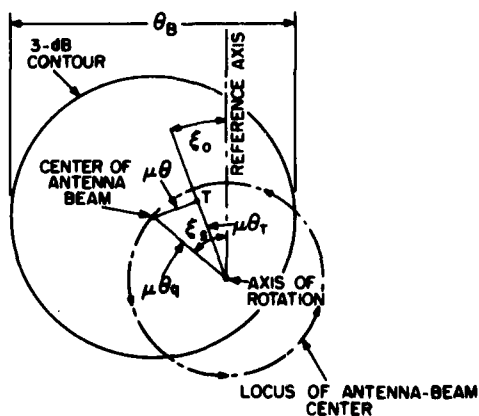

Figure 4. Head-on View of Conical-scan Antenna Beam (After: Skolnik[9])

12

defined by $I_n(x) = i^{-n}J_n(ix)$, where $J_n(x)$ is called the Bessel coefficient of order n, and i is the complex integer. Using eqn. (16), one can write (15) as

$$G'(t) = \exp[-a^2(\theta_q^2 + \theta_T^2)/2] \left[I_o(a^2\theta_q\theta_T) + 2 \sum_{n=1}^{\infty} I_n(a^2\theta_q\theta_T)\cos(n\omega_s t - n\xi_o) \right], \quad (17)$$

with $\omega_s t$ being substituted for ξ_s, where $\omega_s = 2\pi f_s$. To simplify the algebra, let

$$K'' = \left\{ \exp[-a^2(\theta_q^2 + \theta_T^2)/2] \right\} I_o(a^2\theta_q\theta_T) \quad (18)$$

and

$$K_n = \frac{2I_n(a^2\theta_q\theta_T)}{I_o(a^2\theta_q\theta_T)} . \quad (19)$$

With these simplifications, the scanning function (17) becomes

$$G'(t) = K'' \left[1 + \sum_{n=1}^{\infty} K_n \cos(n\omega_s t - n\xi_o) \right] . \quad (20)$$

Expression (20) is somewhat complex but it does show that the antenna scanning function consists of a series which is similar to a Fourier series. There are terms which can be identified as dc, first-harmonic, second-harmonic and so on.

4. RADAR ERROR VOLTAGE AND SETTLING FUNCTION

In order to derive the radar error signal $|V_T|$, one must find the amplitude of eqn. (9). The amplitude can be obtained by quadrature demodulation and low-pass filtering. The results of detection of V_T, or more conveniently V_T/KE_o, is most easily found by writing V_T/KE_o in terms of its in-phase I and quadrature – phase Q components

$$\frac{V_T}{KE_o} = [L + M\cos\phi + N\cos2\phi]\cos\omega t + [M\sin\phi + N\sin2\phi]\sin\omega t. \quad (21)$$

It follows from eqn. (21) that

$I = L + M\cos\phi + N\cos2\phi$

$Q = M\sin\phi + N\sin2\phi$

The amplitude of eqn. (21) is given by

$$\frac{|V_T|}{KE_o} = [I^2 + Q^2]^{\frac{1}{2}}. \quad (22)$$

If the expressions for I and Q are substituted into eqn. (22) and double angle trigometric relations are used, one obtains

$$\frac{\left|V_T\right|}{KE_o} = [L^2 + M^2 + N^2 + 2LM \cos\phi + 2LN \cos2\phi + 2MN \cos\phi]^{\frac{1}{2}}. \qquad (23)$$

4.1 GENERAL SOLUTION

One would wish to express eqn. (22) as a function of terms which are separable rather than being lumped together in an argument of a square root function. Let us try an expression of the form

$$\frac{\left|V_T\right|}{KE_o} = X + Y \cos\phi + Z, \qquad (24)$$

where X, Y and Z are unknowns.

Upon squaring eqn. (24) one obtains

$$\left\{\frac{\left|V_T\right|}{KE_o}\right\}^2 = X^2 + Z^2 + 2XZ + 2Y(X+Z)\cos\phi + Y^2 \cos^2\phi. \qquad (25)$$

The identity $\cos2\phi = 2\cos^2\phi-1$ is substituted into eqn. (23) so that eqn. (23) is expressed in terms of $\cos\phi$ and $\cos^2\phi$. If the constant term and coefficients of the terms in $\cos\phi$ and $\cos^2\phi$ in eqns. (23) [modified] and (25) are equated, the following are obtained:

$$(X+Z)^2 = (L+N)^2 + M^2 - 4LN$$

$$Y(X+Z) = M(L+N)$$

$$Y^2 = 4LN$$

The similarity between the two sides of the second equation might lead one to guess that the values of the unknowns X, Y and Z are: X=L, Y=M and Z=N. If this choice of values is valid it then follows from the first equation that the identity

$$M^2-4LN = 0 \qquad (26)$$

must also be valid. By direct substitution in eqn. (26) of eqns. (10), (11) and (12) one can easily demonstrate that eqn. (26) is always valid. As a final test of our choice for the values of X, Y and Z, the last equation must also be a valid identity. By comparing eqn. (26) and the last equation one can see that it is indeed valid. Therefore, eqn. (24) is a valid expression for eqn. (23) with X=L, Y=M and Z=N. Substitution of these values into eqn. (24) gives the sought after solution

$$\frac{|V_T|}{KE_o} = L + M \cos\phi + N. \tag{27}$$

As a final check, it can be shown that the square of eqn. (27) can be written, with the use of eqn. (26), in a form identical to the square of eqn. (23).

4.2 GAUSSIAN-BEAM SCANNING FUNCTION SOLUTION

If one uses eqn. (20) as the antenna scanning function in eqns. (10), (11) and (12) and subscripts or superscripts, d(direct) and i(indirect), the constants in eqn. (27) are defined as being

$$L = (K''_d)^2 \left[1 + \sum_{n=1}^{\infty} K_n^d \cos(n\omega_s t - n\xi_d) \right]^2 ,$$

$$M = 2\rho K''_d K''_i \left[1 + \sum_{n=1}^{\infty} K_n^d \cos(n\omega_s t - n\xi_d) \right] \left[1 + \sum_{n=1}^{\infty} K_n^i \cos(n\omega_s t - n\xi_i) \right] ,$$

and

$$N = \rho^2 (K''_i) \left[1 + \sum_{n=1}^{\infty} K_n^i \cos(n\omega_s t - n\xi_i) \right] .$$

By substituting these constants into eqn. (27) and making use of the identity $\cos A \cos B = 1/2[\cos(A+B)+\cos(A-B)]$ we obtain

$$\frac{|V_T|}{KE_o} = (K''_d)^2 \left\{ 1 + 2 \sum_{n=1}^{\infty} K_n^d \cos(n\omega_s t - n\xi_d) + \sum_{n=1}^{\infty} \sum_{\ell=1}^{\infty} \frac{K_n^d K_\ell^d}{2} \right.$$

$$\left. \left[\cos\{(n+\ell)\omega_s t - \xi_d(n+\ell)\} + \cos\{(n-\ell)\omega_s t - \xi_d(n-\ell)\} \right] \right\}$$

$$+ 2\rho K'_d K''_i \cos \left\{ 1 + \sum_{n=1}^{\infty} K_n^d \cos(n\omega_s t - n\xi_d) \right.$$

$$+ \sum_{n=1}^{\infty} K_n^i \cos(n\omega_s t - n\xi_i) + \sum_{n=1}^{\infty} \sum_{\ell=1}^{\infty} \frac{K_n^i K_\ell^i}{2}$$

$$\left. \left[\cos\{(n+\ell)\omega_s t - (n\xi_d + \ell\xi_i)\} + \cos\{(n-\ell)\omega_s t - (n\xi_d - \ell\xi_i)\} \right] \right\}$$

$$+ \rho^2 (K''_i)^2 \left\{ 1 + 2 \sum_{n=1}^{\infty} (-1)^n K_n^i \cos(n\omega_s t - n\xi_i) + \sum_{n=1}^{\infty} \sum_{\ell=1}^{\infty} \frac{K_n^i K_\ell^i}{2} \right.$$

$$\left[\cos\{(n+\ell)\omega_s t-(n+\ell)\xi_i\} + \cos\{(n-\ell)\omega_s t-(n-\ell)\xi_i\}\right]\Bigg\}. \tag{28}$$

In the demodulation process $|V_T|/KE_O$ is low-pass filtered with a filter whose cut-off frequency $f_s = \omega_s/2\pi$. Taking the filtering into account and retaining only first-order terms in eqn. (28) we obtain

$$\frac{|V_T|}{KE_O} \approx (K_d'')^2 \left\{1 + \frac{(K_1^d)^2}{2}\right\} + (K_d'')^2 \left\{\left[2K_1^d + K_2^d K_1^d\right] \cos(\omega_s t-\xi_d)\right\}$$

$$+ 2\rho K_d'' K_i'' \cos\phi \left\{1 + \frac{K_1^d K_1^i}{2}\right\} + 2 K_d'' K_i'' \cos\phi \left\{K_1^d \cos(\omega_s t-\xi_d)\right.$$

$$+ K_1^i \cos(\omega_s t-\xi_i) + \frac{K_2^d K_1^i}{2} \cos[\omega_s t-(2\xi_d-\xi_i)] + \frac{K_1^d K_2^i}{2} \cos[\omega_s t-(\xi_d-2\xi_i)]\right\}$$

$$+ \rho^2 (K_i'')^2 \left[1 + \frac{(K_1^i)^2}{2}\right] + \rho^2 (K_i'')^2 \left[2K_1^i + K_2^i K_1^i\right] \cos(\omega_s t-\xi_i). \tag{29}$$

The normalized radar error signal $|V_T|_N$ is derived from eqn. (29) by multiplying through by KE_O and separating the ac and dc terms. The signal $|V_T|_N$ consists of a ratio whose numerator is comprised of the ac terms and denominator is comprised of the dc terms, thus

$$|V_T|_N \cong \frac{\begin{aligned}&(K_d'')^2[2K_1^d+K_1^d K_2^d]\cos(\omega_s t-\xi_d) + 2\rho K_d'' K_i'' \cos\phi\Big\{K_1^d \cos(\omega_s t-\xi_d)\\ &+ K_1^i \cos(\omega_s t-\xi_i) + \frac{K_2^d K_1^i}{2} \cos[\omega_s t-(2\xi_d-\xi_i)] + \frac{K_1^d K_2^i}{2} \cos[\omega_s t-(\xi_d-2\xi_i)]\Big\}\\ &+ \rho^2 (K_i'')^2[2K_1^i+K_2^i K_1^i]\cos(\omega_s t-\xi_i)\end{aligned}}{(K_d'')^2\left[1 + \frac{(K_1^d)^2}{2}\right] + 2\rho K_d'' K_i'' \cos\phi \left[1 + \frac{K_1^d K_1^i}{2}\right] + \rho^2 (K_i'')\left[1 + \frac{(K_1^i)^2}{2}\right]} \tag{30}$$

Note that the parameter KE_O, which contains factors describing the strength of the radar echo, has disappeared. Its disappearance is due to its being a common factor in both the numerator and denominator of eqn. (30). Equation (30) is therefore independent of the amplitudes of the direct and indirect signals and is a function only of their angles-of-arrival and phase difference. For only one target, eqn. (30) would solely be a function of the signal's angle-of-arrival.

The radar signal represented by eqn. (30) is fed into two error angle detectors. These detectors are phase sensitive detectors and yield elevation and azimuth antenna pointing-angle information. The outputs of the detectors are used to drive servo-motors which control the elevation and azimuth of

16

the radar antenna. The conical-scan radar achieves pointing-angle equilibrium when the detector outputs are reduced to zero, which for a single target would be achieved only if the antenna rotation axis was pointed directly at the target. In the elevation error angle detector, eqn. (30) is multiplied by $\cos\omega_s t$* and in the azimuth error detector it is multiplied by $\sin\omega_s t$.

When eqn. (30) is multiplied by $\cos(\omega_s t)$, low pass filtered so that only d-c and near a-c terms remain the result is described by

$$
\epsilon_c^E \cong \frac{\begin{array}{l} \dfrac{(K_d'')^2}{2}[2K_1^d + K_1^d K_2^d]\cos\xi_d + \rho K_d''K_1'' \cos\phi\Big\{K_1^d \cos\xi_d + K_1^i \cos\xi_i \\[2mm] + \dfrac{K^d K^i}{2}\cos(2\xi_d-\xi_i) + \dfrac{K_1^d K_2^i}{2}\cos(\xi_d-2\xi_i)\Big\} + \rho^2 \dfrac{(K_1'')^2}{2}[2K_1^i + K_2^i K_1^i]\cos\xi_i \end{array}}{(K_d'')^2\left[1 + \dfrac{(K_1^d)^2}{2}\right] + 2\rho K_d''K_1'' \cos\phi\left[1 + \dfrac{K_1^d K_1^i}{2}\right] + \rho^2(K_1'')^2\left[1 + \dfrac{(K_1^i)^2}{2}\right]}
$$ (31)

where, ϵ_c^E is called the radar elevation error signal.

Similarly, if eqn. (29) is multiplied by $\sin\omega_s t$ and low-pass filtered the azimuth radar error signal ϵ_c^A is

$$
\epsilon_c^A \cong \frac{\begin{array}{l} \dfrac{(K_d'')^2}{2}[2K_1^d + K_1^d K_2^d]\sin\xi_d + \rho K_d''K_1'' \cos\phi\Big\{K_1^d \sin\xi_d + K_1^i \sin\xi_i \\[2mm] + \dfrac{K_2^d K_1^i}{2}\sin(2\xi_d-\xi_i) + \dfrac{K_1^d K_2^i}{2}\sin(\xi_d-2\xi_i)\Big\} + \rho^2 \dfrac{(K_1'')^2}{2}[2K_1^i + K_2^i K_1^i]\sin\xi_i \end{array}}{(K_d'')^2\left[1 + \dfrac{(K_1^d)^2}{2}\right] + 2\rho K_d''K_1'' \cos\phi\left[1 + \dfrac{K_1^d K_1^i}{2}\right] + \rho^2(K_1'')^2\left[1 + \dfrac{(K_1^i)^2}{2}\right]}
$$ (32)

If a further omission of higher order terms, such as $K_1^d K_2^d$, is made in eqns. (31) and (32) they become

$$
\epsilon_c^E \cong \frac{(K_d'')^2 K_1^d \cos\xi_d + \rho K_d''K_1'' \cos\phi\Big\{K_1^d \cos\xi_d + K_1^i \cos\xi_i\Big\} + \rho^2(K_1'')^2 K_1^i \cos\xi_i}{(K_d'')^2\left[1 + \dfrac{(K_1^d)^2}{2}\right] + 2\rho K_d''K_1'' \cos\phi\left[1 + \dfrac{K_1^d K_1^i}{2}\right] + \rho^2(K_1'')^2\left[1 + \dfrac{(K_1^i)^2}{2}\right]}
$$ (33)

and

$$
\epsilon_c^A \cong \frac{(K_d'')^2 K_1^d \sin\xi_d + \rho K_d''K_1'' \cos\phi\Big\{K_1^d \sin\xi_d + K_1^i \sin\xi_i\Big\} + \rho^2(K_1'')^2 K_1^i \sin\xi_i}{(K_d'')^2\left[1 + \dfrac{(K_1^d)^2}{2}\right] + 2\rho K_d''K_1'' \cos\phi\left[1 + \dfrac{K_1^d K_1^i}{2}\right] + \rho^2(K_1'')^2\left[1 + \dfrac{(K_1^i)^2}{2}\right]}
$$ (34)

*Note: Skolnik[9] /p. 173, eqn. (5.12) and (5.13)/ has mistakenly identified the $\cos\omega_s t$ term with the azimuth error and the $\sin\omega_s t$ term with the elevation error.

All of the approximations made in deriving eqns. (33) and (34) have involved omitting terms in the amplitudes of the cosine functions in eqn. (20) with n>1. In Section 7 we will see that for small target error angles the omitted terms are considerably smaller than those that are retained. Therefore it will be seen that the approximations made in arriving at eqns. (33) and (34) are justified.

4.2.1 Radar Settling Function

The numerator of eqn. (33) is called the conical-scan elevation settling function, F_c. It has importance to this work because it defines the equilibrium elevation pointing angle for the radar antenna. The radar's elevation servo-system is designed such that it achieves a state of equilibrium only when the error angle voltage ϵ_c^E becomes zero, which is defined by the condition $F_c=0$. The radar elevation settling function is given by

$$F_c \cong K_1^d \, (K_d'')^2 \, \cos\xi_d + \rho K_d'' K_1'' \, \cos\phi \, [K_1^d \, \cos\xi_d + K_1^i \, \cos\xi_i] + \rho^2 (K_1'')^2 \, K_1^i \, \cos\xi_i. \quad (35)$$

5. COMPARISON OF CONICAL-SCAN AND MONOPULSE RADARS

In Section 5 analytical results derived in Section 4.2 are compared with equations describing the low-angle behavior of monopulse radars. For convenience a derivation of the monopulse equations is given in Appendix A.

5.1 EQUIVALENCE BETWEEN MONOPULSE AND CONICAL-SCAN RADARS

The settling function for a monopulse radar[15] (numerator of eqn (A6)) is

$$F_M = g_{\Delta d} g_{\Sigma d} + \rho (g_{\Delta d} g_{\Sigma i} + g_{\Delta i} g_{\Sigma d}) \, \cos\phi + \rho^2 g_{\Delta i} g_{\Sigma i} \quad (36)$$

where $g_{\Delta d}$ = gain of the difference beam for the direct signal

         $g_{\Sigma d}$ = gain of the sum beam for the direct signal

         $g_{\Delta i}$ = gain of the difference beam for the indirect signal

         $g_{\Sigma i}$ = gain of the sum beam for the indirect signal

The form of the settling function of the conical-scan radar (eqn. (35)) is very similar to that for a monopulse radar (eqn. (36)). This agreement suggests a similarity in their low-angle tracking behavior.

If one is interested only in describing the normal elevation angle tracking behavior for conical-scan and monopulse radars, absolute antenna gains need not be specified when using eqns. (35) and (36). In either case, the equilibrium or settling angle is defined by setting the scanning function equal to zero. Therefore, only relative antenna gain need be measured for determining their low-angle target tracking behavior.

18

5.2 MONOPULSE TRANSFORMATIONS

It follows from a term-by-term comparison of eqns. (35) and (36) that a conical-scan radar can be treated as a monopulse radar provided one makes the following transformations.

$$K_d'' \rightarrow g_{\Sigma d} \tag{37}$$

$$K_d'' K_1^d \cos\xi_d \rightarrow g_{\Delta d} \tag{38}$$

$$K_1'' \rightarrow g_{\Sigma i} \tag{39}$$

$$K_1'' K_1^i \cos\xi_i \rightarrow g_{\Delta i} \tag{40}$$

These transformations assume that the radar target is well behaved with a cross-section that is constant or varies only slowly with time. Rapidly varying targets may have a component of their fluctuations which causes a modulation of frequency f_s to appear on the radar signal and to be erroneously interpreted as target tracking information.

For defining the low-angle tracking behavior of conical-scan radars, the parameters in eqns. (37)-(40) can be derived in two ways. First, they can be evaluated directly from the expressions given in Section 3.2, which were derived for a Gaussian approximation to the antenna pattern. Secondly, as will be shown in Section 5.2, they can be derived directly from the measured antenna pattern.

5.3 MONOPULSE EQUIVALENT ERROR SIGNAL

When the transformations given by eqns. (37) to (40) are substituted into eqn. (33) it takes the form

$$\epsilon_c^E \cong \frac{g_{\Delta d} g_{\Sigma d} + \rho\cos\phi \left\{ g_{\Delta d} g_{\Sigma i} + g_{\Sigma d} g_{\Delta i} \right\} + \rho^2 g_{\Sigma i} g_{\Delta i}}{g_\Sigma^2 \left[1 + \frac{(K_1^d)^2}{2} \right] + 2\rho g_{\Sigma d} g_{\Sigma i} \cos\phi \left[1 + \frac{K_1^d K_1^i}{2} \right] + \rho^2 g_{\Sigma i} \left[1 + \frac{(K_1^i)^2}{2} \right]}, \tag{41}$$

where ϵ_c^E = error signal.

By means of eqns. (37)-(40), the numerator of eqn. (33) has been rewritten so as to have the same form as the numerator of the comparable monopulse expression given in eqn. (A6). The denominators of the expressions for conical-scan and monopulse error-signals differ by the factors given by the square brackets in eqn. (33) or eqn. (41). To achieve agreement between the denominators of eqns. (41) and (A6), transformations (37) and (39) must be modified to take respectively the forms:

$$g'_{\Sigma d} = K''_d \left[1 + \frac{(K_1^d)^2}{2} \right]^{\frac{1}{2}}$$

$$g'_{\Sigma i} = K''_i \left[1 + \frac{(K_1^i)^2}{2} \right]^{\frac{1}{2}} .$$

For small error angles (deviations of the target line-of-sight with the antenna rotation-axis) the transformations can be written as:

$$g'_{\Sigma d} \cong K''_d \left[1 + \frac{(K_1^d)^2}{4} \right] \qquad (42)$$

$$g'_{\Sigma i} \cong K''_i \left[1 + \frac{(K_1^i)^2}{4} \right] . \qquad (43)$$

A representative value for the second term in the square brackets of eqns. (42) and (43) can be derived using parameters and experimental data for a typical conical-scan radar. Such a result is given by Figure 7(b). It shows a low-angle target signature measured with a Prelort radar. The nominal height of the target was 100 yards.

From Figure 7(b) one can find a maximum value for the target error angles. Taking a range of 25 Kyds, for example, the maximum indicated target height error is approximately 100 yards. This corresponds to an error angle of 0.23°.

From eqn. (19), we find that

$$K_1 = \frac{2 I_1 (a^2 \theta_q \theta_T)}{I_o (a^2 \theta_q \theta_T)}$$

A representative value for the arguments of the modified Bessel functions I_1 and I_0 is

$$a^2 \theta_q \theta_T = \frac{2.776 \times 0.45 \times 0.23}{0.9} = 0.32.$$

From Wylie[16] [p. 359] we find the value of K_1 corresponding to the above argument is 0.3. It follows that the bracketed terms in eqns. (42) and (43) are approximately equal to 1.023. Therefore, for small target error angles, the transformations given by eqns. (42) and (43) are equivalent to those given respectively by eqns. (37) and (39), and eqn. (41) is identical to eqn. (A6).

If one takes advantage of the approximate equality of $g'_{\Sigma d}$ with $g_{\Sigma d}$ and $g'_{\Sigma i}$ with $g_{\Sigma i}$, eqn. (41) can be written as

$$\epsilon_c^E \cong \frac{g_{\Delta d} g_{\Sigma d} + \rho \cos\phi \left\{ g_{\Delta d} g_{\Sigma i} + g_{\Sigma d} g_{\Delta i} \right\} + \rho^2 g_{\Sigma i} g_{\Delta i}}{g_{\Sigma d}^2 + 2\rho g_{\Sigma d} g_{\Sigma i} \cos\phi + \rho^2 g_{\Sigma i}} . \qquad (44)$$

5.4 DIFFERENCES BETWEEN MONOPULSE AND CONICAL-SCAN RADARS

One of the main differences between a monopulse radar and a conical-scan radar is the time taken by each to obtain sensing information. A monopulse radar is capable of tracking a target on a pulse-by-pulse basis, which suggests a maximum sampling rate equal to the prf of the radar. On the other hand, a conical-scan radar needs to process somewhat more than four pulses[9] to track a target. Therefore, for radars with equal prfs, the maximum data rate is greater for monopulse than for conical-scan radars.

The inherently lower data rates of conical-scan radars, do not usually cause their performance to be degraded, per se, compared to that of monopulse radars. Normally, bandwidths of radar servo-systems are much lower than typical prfs. Therefore, the response times for both monopulse and conical-scan radars are usually limited by the response times of their antenna systems. Typically, these are approximately equal.

For low-angle and multiple target tracking, monopulse radars are capable of providing more target information than conical-scan radars. This difference arises from a single fact: the phase of the radar signal is preserved in monopulse radars and discarded in conical-scan radars. Multiple targets affect, not only the amplitude of the radar signal, whether it be a monopulse or conical-scan system, but also its phase. In a monopulse system both the amplitude and phase of the radar signal can be measured because the sum signal is available as a phase reference. Usually, in an operational system, only the in-phase component is measured, but it is possible, by the addition of another IF channel to the radar receiver to also measure the quadrature-phase component. Resolution of radar error signals into in-phase and quadrature-phase components is not possible in a conical-scan system because there is no signal equivalent to a monopulse sum-signal to serve as a reference.

The essential difference between monopulse and conical-scan radars results from the manner in which these two systems receive tracking information. Monopulse radars receive information continuously from two independent beams, whereas conical-scan radars receive information from only one beam whose pointing direction is changing continuously. It follows that conical-scan systems receive information at a lower rate than monopulse radar systems. They can only be considered to be equivalent if the final data rate is slowed sufficiently by integration effects, such as those provided by the inertia of antenna systems, so that their differences do not become apparent. It is only for these lower data rates that a conical-scan radar can be considered to be receiving information from an equivalent split beam and treated as a monopulse radar.

6. MONOPULSE EQUIVALENT TO THE PRELORT RADAR

This section gives an example of the application of the conical-scan radar theory developed in Sections 4 and 5. The example consists of simulating the low-angle tracking behavior of a Prelort radar.

6.1 PRELORT RADAR PARAMETERS

Low-angle data have been obtained, with two conical-scan Prelort tracking radars situated at Primrose Lake, Alberta. These and additional data that were collected in 1979 will be used to test and develop low-angle tracking algorithms. The radars operate in the C-band, are collocated but separated in height by 30 feet. Table 1 lists some pertinent parameters.

6.2 EQUIVALENT MONOPULSE ANTENNA PATTERNS

Before the Primrose Lake data can be used for testing tracking algorithms, mathematical models of the Prelort radars must first be developed. This requires that one measures the radar antenna pattern and then derives the equivalent monopulse antenna patterns. Modelling of the signature or tracking behavior of a monopulse radar with low-angle targets is rather straightforward once the sum and difference antenna patterns are known. It is simply a matter of applying vector arithmetic to vectors whose magnitude and phase are determined by antenna gains, coefficients of reflection and curved earth geometry.

TABLE 1

Prelort Radar Parameters

(i)   Antenna height (above surface of water) —   293 feet (Radar 2)
                                                   323 Feet (Radar 1)

(ii)   Frequency — variable, C-band, 5450–5825 MHz

(iii) Antenna scan rate — 30 Hz

(iv)   Antenna — 14 ft. disc reflector
               sidelobe level 20 dB
               beamwidth — 0.9°
               polarization, left and right hand   } selectable by the operator
               circular, vertical and horizontal linear
               squint angle — 0.45°

(v)   PRF — variable, 160, 320, and 640 pulses per second

(vi)   Pulsewidth — 0.25, 0.5 and 1.0 μsec

(vii) Output power — 250 kw peak

(viii) Range resolution — better than one yard*

(ix)   *Tracking range (beacon target)* — 500 yards to 2000 nmi

(x)   Tracking range (aircraft target) — 100 nmi

* *Using Split-gate Time Discrimination Techniques (see Barton and Ward[4], pp. 72–78)*

When deriving equivalent monopulse antenna patterns for a conical-scan radar, one should treat the numerator and denominator of eqn. (41) independently. The numerators of eqns. (41) and (A6) are obviously equal. The equivalence of their denominators is not as straightforward and has required special consideration. We are primarily interested in deriving equivalent patterns for the *numerator of eqn. (41)* because it is the expression from which the settling function is derived and which defines the equilibrium pointing angle for the radar. For small error-angles it was found that the square bracketed factors in the denominator of eqn. (41) are approximately equal to one. As concluded earlier, when dealing with small error angles, eqns. (41) and (A6) can therefore be considered to be mathematical equivalents. It follows that the equivalent patterns expressly derived here for the numerator of eqn. (41) are also applicable to the whole of eqn. (41).

Equation (20) shows that the dc and first ac components of the radar scanning function are respectively K'' and $K''K_1$. The equivalent sum patterns are, according to eqns. (37) and (39), given by the dc component of the antenna scanning function. Equations (38) and (40) imply that the equivalent difference pattern would be given by the first ac component of the antenna scanning function if $|\cos\xi| \simeq 1$. Measurements of the low-angle tracking behavior of conical-scan radars show that the azimuth error angles are less than 0.18 times the elevation error angles. The ratio of elevation to azimuth deviations suggests that ξ departs by no more than $10°$ from $0°$ or $180°$. Therefore, to a good approximation $|\cos\xi| \simeq 1$ and the equivalent difference pattern is equal to the first ac component of the antenna scanning function.

The Prelort radar's antenna pattern has not yet been measured. In the interim it is assumed that its pattern can be represented by a typical radar antenna pattern. In Figure 5 is shown a typical instantaneous conical-scan beam pattern, comprised of the beam at the extremes of its vertical motion during one cycle of its rotation. Each pattern in Figure 5 is synthesized from a weighted sum of five sin x/x functions. The sin x/x functions are separated in angle by π radians, so that, peaks and first nulls of neighboring functions are coincident. The patterns in Figure 5 have beamwidths of $0.9°$ and are separated by $0.9°$. The level of the first sidelobes is -26 dB, which is lower than specified in Table 1, but otherwise it is expected that these patterns will serve as a good approximation to the Prelort radar patterns.

In Figure 6 we are given equivalent monopulse patterns derived from the patterns in Figure 5. They were calculated from antenna scanning functions derived for a series of target error angles. The scanning functions were calculated directly from the patterns in Figure 5 by means of a graphical technique described in Section 7.

Harmonic analysis techniques were used to derive the dc components of the antenna scanning functions. The dc components define the equivalent sum pattern. Rather than continue with harmonic analysis, for deriving the equivalent difference pattern, it was found to be simpler to use the instantaneous patterns in Figure 5 and by subtraction derive the patterns directly. It was seen in Figure 2 that the amplitude of the time varying portion of the antenna scanning function is nearly equal to one-half the difference in gains of the instantaneous patterns. If the scanning function is sinusoidal, or in other words its harmonic content low, the parameter A_1 in Figure 2 is nearly equal to the amplitude of the first ac component of the antenna scanning

function. In Section 7 it will be shown that the first harmonic of the antenna scanning function is the predominant time-varying component.
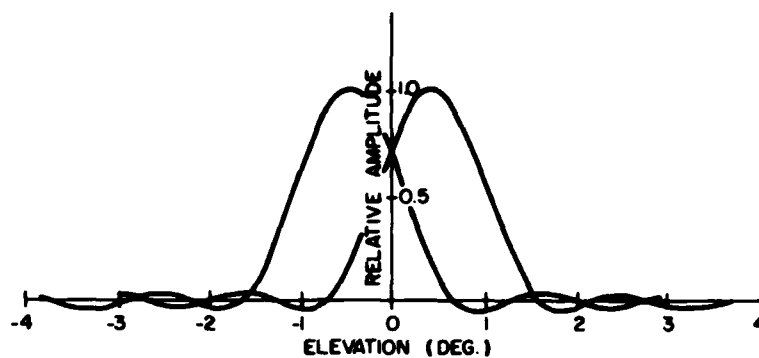

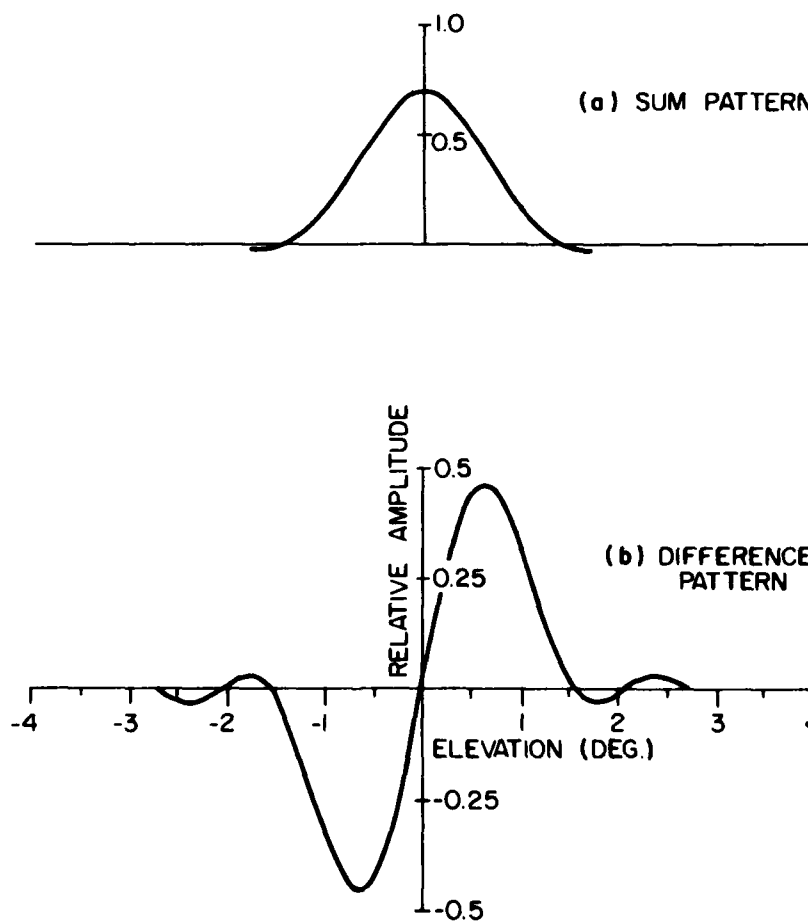*Figure 5. Typical Radar Antenna Patterns Separated by One-half of a Beamwidth*

(a) SUM PATTERN

(b) DIFFERENCE PATTERN

Figure 6. Equivalent Monopulse Sum and Difference Patterns for the Prelort Conical-scan Radar

6.3 MEASURED CONICAL-SCAN RADAR SIGNATURE

Figure 7(a) gives a simulation of the low-angle tracking behavior of a conical-scan radar tracking a target whose nominal height is 100 yards. It was derived from a software model of a monopulse radar using the equivalent patterns given in Figure 6. The measured behavior (signature) of the Prelort radar for the same target profile is shown in Figure 7(b).
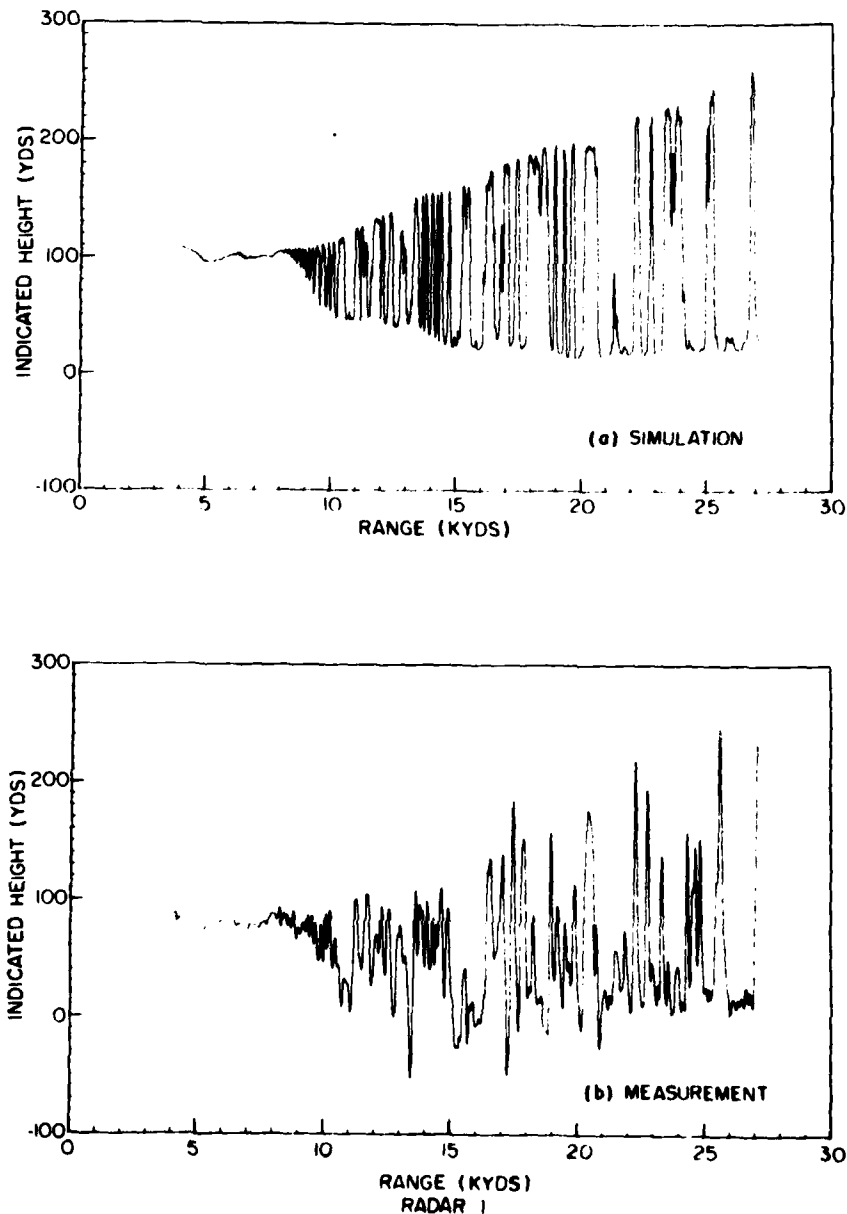

Figure 7. Comparison of Simulated and Measured Low-angle Conical-scan Radar Data

The agreement between the two results in Figure 7 is reasonable. Discrepancies can be explained as being due to factors other than the use of the equivalent monopulse patterns in modelling the Prelort radar. The dominant source of error in the simulated result is attributed to the measurement of target height. The simulated data were derived for a target profile measured independently of the radar. Measurements were made by both a sensitive barameter located in the target aircraft and a system of ground-based phototheodolites. The maximum discrepancy between target heights measured by these two systems of instruments was about 3.3 yards.

Small deviations in target height can have a large effect on the radar's tracking behavior. For example, a change in target height of 3.3 yards for a target at a height of 100 yards and a range of 20 Kyds produces a change of 360° in Φ. In other words, the target height measured by the radar can vary through a complete cycle, consisting of a null and a peak, with as small a change in target height as that quoted above. The radar output is therefore a very sensitive function of target height and range. Since the target height was only known to an accuracy of ±1.5 yards it follows that the discrepancies between Figures 7(a) and 7(b) can be accounted for, soley by inaccuracies in target height.

7. EXAMPLES OF ANTENNA SCANNING FUNCTIONS

Typical antenna scanning functions are presented in Section 7 which are derived for a Prelort radar. It will be shown that for target error angles that are likely to be encountered in practice, the first-harmonic of the Fourier series representation for these functions is dominant. This result will permit us to conclude that the linear conical-scan theory developed in this report accurately describes the low-angle tracking behavior of conical-scan radars.

7.1 TYPICAL ANTENNA SCANNING FUNCTION

Let us now calculate a typical antenna scanning function for the antenna pattern given in Figure 5 and for

$$\theta_q = 0.45°$$

$$\theta_T = 0.25°$$

First, one calculates the angle of offset of the target axis with respect to the centre of the beam. The pertinent parameters and geometry required for this calculation are defined in Figure 8, where we are given a head-on view of the antenna, which is shown as a contour map of relative amplitude. The dashed circle represents the path of the target around the antenna rotation axis. Actually it is the antenna beam that rotates and the target that is stationary, but it is more convenient to formulate the problem in terms of a stationary antenna and rotating target. From a mathematical point of view the two are equivalent.

26

Applying the same reasoning used in deriving eqn. (14) to the geometry
shown in Figure 8 and the law of cosines one can write the expression for the
off-beam-centre angle θ as

$$\theta = [(\theta_T)^2 + (\theta_q)^2 - 2\theta_q\theta_T \cos\omega_s t]^{\frac{1}{2}}. \tag{45}$$

Using eqn. (45) to solve for θ with the parameters listed above, we can
derive a typical antenna scanning function for the pattern given in Figure 5.
The result is given in Figure 9. The scanning function's general form can be
verified by comparing it with the contour lines intercepted by the target
path in Figure 8. As would be expected from the uniform spacing of the
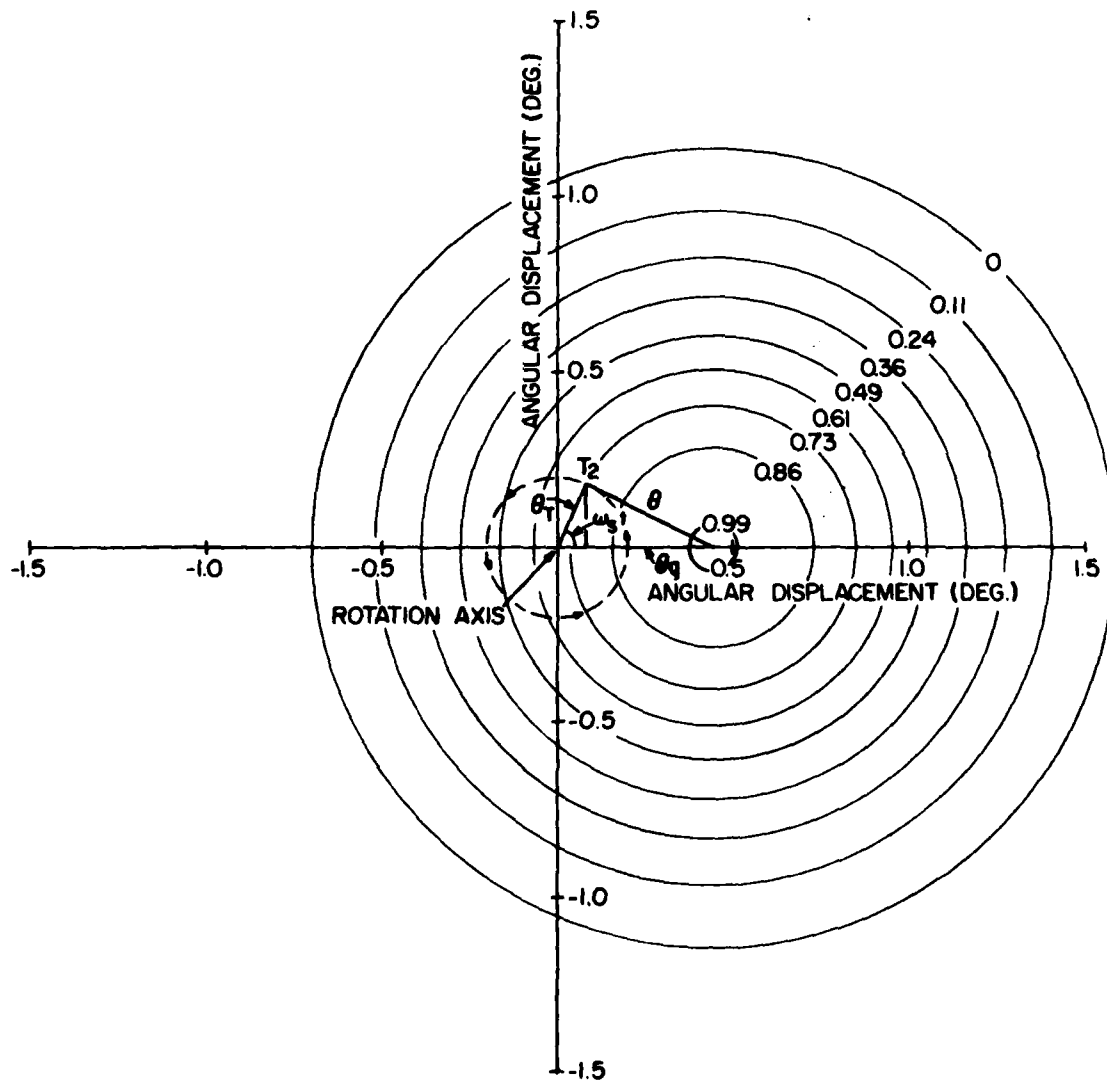contour lines in Figure 8 the scanning function is quite a good sinusoid.

Figure 8. Head-on View of the Antenna Beam Shown as a Contour Plot of Constant Relative Amplitude.
A Target Path has been Sketched in to Derive a Typical Scanning Function.

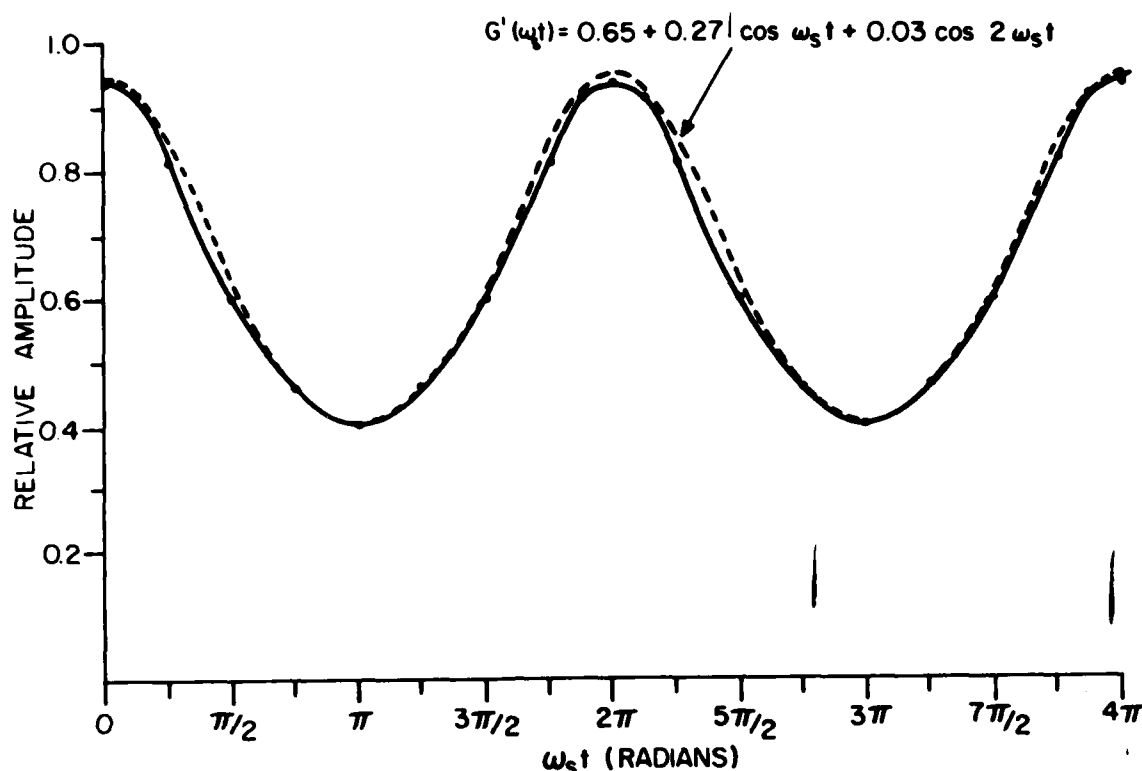$$G'(\omega_s t) = 0.65 + 0.27 |\cos \omega_s t| + 0.03 \cos 2\omega_s t$$

Figure 9. Comparison of an Antenna Scanning Function for $\theta_T = 0.25$ Degrees (Dashed Curve) and a Function (Solid Curve) Comprised of Harmonics of the Radar Scanning Frequency ω_s

7.2 HARMONIC ANALYSIS

We now carry out a harmonic analysis of the antenna scanning function given in Figure 9. Consider an even function $g(t)$ whose period is $2p$. Its Fourier coefficient a_n is given by

$$a_n = \frac{2}{p} \int_0^p g(t) \cos \frac{n\pi t}{p} \, dt. \tag{46}$$

The integration may be performed numerically using the trapezoidal rule. If for convenience we take $\Delta t = p/8$, eqn. (46) can be written as

$$a_n = \frac{2}{p} \left[\frac{p}{8} \left(\frac{g_0}{2} \cos \left(\frac{n\pi}{p} \cdot 0 \right) + g_1 \cos \left(\frac{n\pi}{p} \frac{p}{8} \right) + \cdots + g_7 \cos \left(\frac{n\pi}{p} \frac{7p}{8} \right) + g_8 \cos \left(\frac{n\pi}{p} p \right) \right) \right]$$

or

$$a_n = \frac{1}{4} \left[\frac{g_0}{2} + g_1 \cos \frac{n\pi}{8} + \cdots + g_7 \cos \frac{7n\pi}{8} + \frac{g_8}{2} \cos n\pi \right] \tag{47}$$

where $g_0, g_1, g_2, \ldots, g_8$, are the values of g at $t=0$, t, $2\Delta t, \ldots, 8\Delta t$.

The function g(t) can be written as

$$g(t) = \frac{a_0}{2} + a_1 \cos\omega t + a_2 \cos 2\omega t + a_3 \cos 3\omega t + a_4 \cos 4\omega t + a_5 \cos 5\omega t + \cdots \quad (48)$$

The coefficients of a_n are tabulated in Table 2 for the antenna scanning function in Figure 9. Using these coefficients the scanning function is calculated to be

$$G'(\omega_s t) = 0.65 + 0.27 \cos\omega_s t + 0.03 \cos 2\omega_s t + 0.03 \cos 3\omega_s t + 0.0025 \cos 4\omega_s t$$

$$- 0.0019 \cos 5\omega_s t + \cdots . \quad (49)$$

The harmonic terms in eqn. (49) are small compared with the fundamental. If eqn. (49) is truncated and only three terms retained it remains a very close approximation to the antenna scanning function, as demonstrated in Figure 9. If only two terms were retained it would still remain a good approximation.

One can now define the necessary conditions for the validity of eqn. (33) more succinctly. Simply stated, if the radar antenna scanning function can be approximated by the first two terms of its Fourier series, eqn. (33) accurately describes the behavior of a conical-scan radar tracking a low-angle target. Since eqn. (33) was used as the basis for defining equivalent monopulse patterns, the accuracy of this representation for a conical-scan radar is determined by how closely the ac term of the antenna scanning function resembles a sinusoid.

TABLE 2

Fourier Coefficients for the Antenna Scanning Function in Figure 9

n	0	1	2	3	4	5
$\frac{g_0}{2}$	0.47	0.47	0.47	0.47	0.47	0.47
$g_1 \cos \frac{n\pi}{8}$	0.92	0.82	0.65	0.35	0	-0.352
$g_2 \cos \frac{n\pi}{4}$	0.82	0.58	0	-0.58	-0.82	-0.579
$g_3 \cos \frac{3n\pi}{8}$	0.73	0.28	-0.52	-0.67	0	0.674
$g_4 \cos \frac{n\pi}{2}$	0.62	0	-0.62	0	0.62	0
$g_5 \cos \frac{5n\pi}{8}$	0.51	-0.20	-0.36	0.47	0	-0.508
$g_6 \cos \frac{3n\pi}{4}$	0.46	-0.33	0	0.33	-0.46	0.326
$g_7 \cos \frac{7n\pi}{8}$	0.42	-0.39	0.30	-0.6	0	0.161
$\frac{g_8}{2} \cos n\pi$	0.20	-0.20	0.20	-0.20	0.20	-0.20

7.3 FURTHER EXAMPLES

Figure 10 gives antenna scanning functions for a number of values of target error angle θ_T. They start off being nearly sinusoidal for small values of θ_T but become increasingly distorted as θ_T increases. A visual inspection of Figure 10 suggests that the harmonic content of the antenna scanning functions increase rapidly for values of θ_T greater than about 0.4°.

It is thought that the accuracy of the results obtained by applying the monopulse transformations [eqns. (37) to (40)] to conical-scan radars will vary inversely with the level of harmonic distortion in the antenna scanning function. When applied to the Prelort radar, these transformations are expected to give good results for θ_T less than 0.4° and results that become increasingly inaccurate as θ_T becomes greater than 0.4°. Although the results given in Figure 7(b) show values for $|\theta_T|$ as high as 0.66°, there is a tendency for the maxima of $|\theta_T|$ to be less than 0.42°. Therefore, it is thought that the Prelort radar operated almost entirely within its linear region. There- fore, the radar's behavior is thought to have been accurately described by the monopulse transformations. The result in Figure 7(b) is probably typical for a conical-scan radar tracking a low-angle target. Therefore, it appears that the monopulse transformation technique for describing the behavior of conical- scan radars with low-angle targets should have fairly widespread applicability.
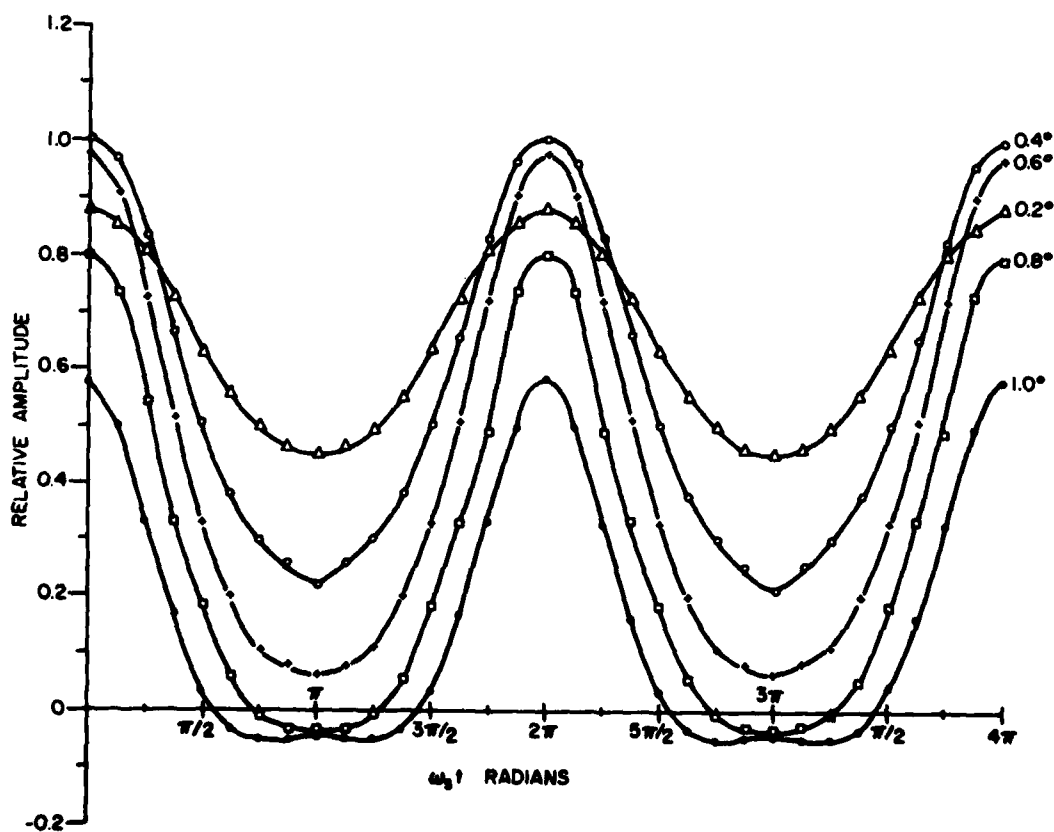

Figure 10. Family of Antenna Scanning Functions. The Value of θ_T is Indicated Along Side Each Curve.

8. SUMMARY

This report has dealt with the problem of describing the behavior of conical-scan radars tracking low-angle targets. Our approach has consisted of demonstrating an equivalence between conical-scan and monopulse radars and then using the better developed monopulse theory for describing the behavior of conical-scan radars. This approach greatly simplifies the problem of developing a theory for the low-angle behavior of conical-scan radars. The resulting theory, summarized by eqn. (44), is a first-order theory applicable only for small target error-angles. If greater accuracy is required one needs to solve the slightly more complex equations [eqns. (31) and (32)] using numerical techniques.

Some example antenna scanning functions were derived for a simulated conical-scan antenna pattern. It was found that their harmonic content was low for target error angles less than one-half of a BW. It follows that the conical-scan radar theory based on monopulse transformations, is also probably valid for target error angles less than about 0.5 BW. Since the example experimental data exhibited maximum target angles that were generally less than 0.5 BW, it is thought that the theory presented in this report is probably adequate for describing the low-angle tracking behavior of conical-scan radars.

9. ACKNOWLEDGEMENT

10. REFERENCES

1. McCreary, T.S., *Summary Report on the Low E Tracking Study*, Vitro Laboratories, Contract N0024-C-70-1192, December 1971.

2. Barton, D.K., *Low-angle Radar Tracking*, Proc. of the IEEE, Vol. 62, No. 6, pp. 687-704, June 1974.

3. Barton, D.K., *Low-angle Tracking*, Microwave Journal, pp. 19-34, December 1976.

4. Barton, D.K. and H.R. Ward, *Hand Book of Radar Measurement*, Prentice-Hall, pp. 142-158, 1969.

5. White, W.D., *Low-angle Radar Tracking in the Presence of Multipath*, IEEE Trans. AES-10, No. 6, pp. 835-852, November 1974.

6. Sherman, S.M., *The Use of 'Complex Indicated Angles' in Monopulse Radar to Locate Unresolved Targets*, Proc. Nat. Electronic Conf., Vol. 22, pp. 243-248, 1966.

7. Linde, G., *Improved Low Elevation Angle Tracking with Use of Frequency Agility*, Technical Memorandum, NRL Radar Division, September 1969.

8. Dax, P.R., *Keet Track of that Low-flying Attack*, Microwaves, pp. 36-53, April 1976.

9. Skolnik, M.I., *Introduction to Radar Systems*, McGraw-Hill Book Company, pp. 164-197, 1962.

10. Dunn, J.H. and D.D. Howard, *Tracking Error Caused by Multipath*, Radar Handbook (M.I. Skolnik ed.), McGraw-Hill Book Company, pp. (28-24)-(28-25), 1970.

11. Fishback, W.T., *Errors in Radar Height Measurements*, Propagation of Short Radio Waves (D.E. Kerr ed.), MIT Rad. Lab. Series, McGraw-Hill Book Company, pp. 436-444, 1951.

12. Damonte, J.R. and Dom. J. Stoddard, *An Analysis of Conical-scan Antennas for Tracking*, IRE Nat. Con. Rec., Vol. 4, pp. 39-47, 1956.

13. Speake, G.D. (Chairman), *The Problems of Low-Angle Radar Tracking in the Presence of Sea Reflections*, NATO Industrial Advisory Sub-Group 4 Document, NIAG(72)(SG/4)D/2, AC/141 (IEG/1)D/71, pp. 19-20, May 1972.

14. Whittaker, E.T. and G.N. Watson, *Modern Analysis*, Fourth edition, p. 347, ex. 3, and p. 372, Cambridge University Press, New York, 1950.

15. Dax, P.R., *Accurate Tracking of Low Elevation Targets over the Sea With a Monopulse Radar*, in Radar - Present and Future, IEE Conf. Publ. No. 105, London, England, 23-25 October 1973, pp. 160-165.

16. Wylie, C.R., *Advanced Engineering Mathematics*, McGraw-Hill Book Co., p. 206, 1966.

A P P E N D I X   A

Monopulse Radar Error Voltage

A derivation of the error voltage for a monopulse radar is presented in Appendix A. In Figure A.1 are given typical monopulse sum and difference patterns. Direct and indirect signals are shown being intercepted by the monopulse antenna patterns.

Expressions for the sum and difference radar voltages for the direct and indirect signals can be written directly from Figure A.1.

$$\Sigma = g_{\Sigma d} \, E_{TT} \, e^{j\omega t} + g_{\Sigma i} \, \rho \, E_{TT} \, e^{j(\omega t + \phi)} \tag{A.1}$$

$$\Delta = g_{\Delta d} \, E_{TT} \, e^{j\omega t} + g_{\Delta i} \, \rho \, E_{TT} \, e^{j(\omega t + \phi)} ; \tag{A.2}$$

where

Σ = Total sum-channel voltage

Δ = total difference-channel voltage

E_{TT} = amplitude of direct signal from the target

$g_{\Delta d}$ = gain of the difference beam for the direct signal

$g_{\Sigma d}$ = gain of the sum beam for the direct signal

$g_{\Delta i}$ = gain of the difference beam for the indirect signal

$g_{\Sigma i}$ = gain of the sum beam for the indirect signal.

The radar error signal ϵ_M is defined as

$$\epsilon_M = \frac{\Delta}{\Sigma} . \tag{A.3}$$

It is called an error signal because in a monopulse radar it is a linear function of the angular displacement of the target from the beam axis. By direct substitution of eqns. (A.1) and (A.2) into eqn. (A.3) we can write

$$\epsilon_M = \frac{g_{\Delta d} g_{\Sigma d} + \rho \cos\phi (g_{\Delta d} g_{\Sigma i} + g_{\Delta i} g_{\Sigma d}) + j\rho \sin\phi (g_{\Delta i} g_{\Sigma d} - g_{\Delta d} g_{\Sigma i}) + \rho^2 g_{\Delta i} g_{\Sigma i}}{g_{\Sigma d}^2 + 2\rho \cos\phi \, g_{\Sigma d} g_{\Sigma i} + \rho^2 g_{\Sigma i}^2} . \tag{A.4}$$

The radar error signal can also be written as

$$\varepsilon_M = \varepsilon_M^I + j \; \varepsilon_M^Q \qquad\qquad (A.5)$$

where

$$\varepsilon_M^I = \frac{g_{\Delta d}g_{\Sigma d} + \rho\cos\phi(g_{\Delta d}g_{\Sigma i}+g_{\Delta i}g_{\Sigma d}) + \rho^2 g_{\Delta i}g_{\Sigma i}}{g_{\Sigma d}^2 + 2\rho\cos\phi \; g_{\Sigma d}g_{\Sigma i} + \rho^2 g_{\Sigma i}^2} \qquad (A.6)$$

and

$$\varepsilon_M^Q = \frac{\rho\sin\phi(g_{\Delta i}g_{\Sigma d} - g_{\Delta d}g_{\Sigma i})}{g_{\Sigma d}^2 + 2\rho\cos\phi \; g_{\Sigma d}g_{\Sigma i} + \rho^2 g_{\Sigma i}^2} \qquad (A.7)$$

The parameters ε_M^I and ε_M^Q are called respectively the in-phase and quadrature-phase components of the elevation radar error signal. Typically, only ε_M^I is derived in a monopulse radar because for a single target and a phase balanced radar receiver $\varepsilon_M^Q \equiv 0$.

If one allows $g_{\Delta i} \to 0$ and $g_{\Sigma i} \to 0$ in eqns. (A.6) and (A.7), the resulting expressions define the radar error signal for a single target. Single target error signals are defined by

$$\varepsilon_M^I = \frac{g_{\Delta d}}{g_{\Sigma d}} \qquad\qquad (A.8)$$
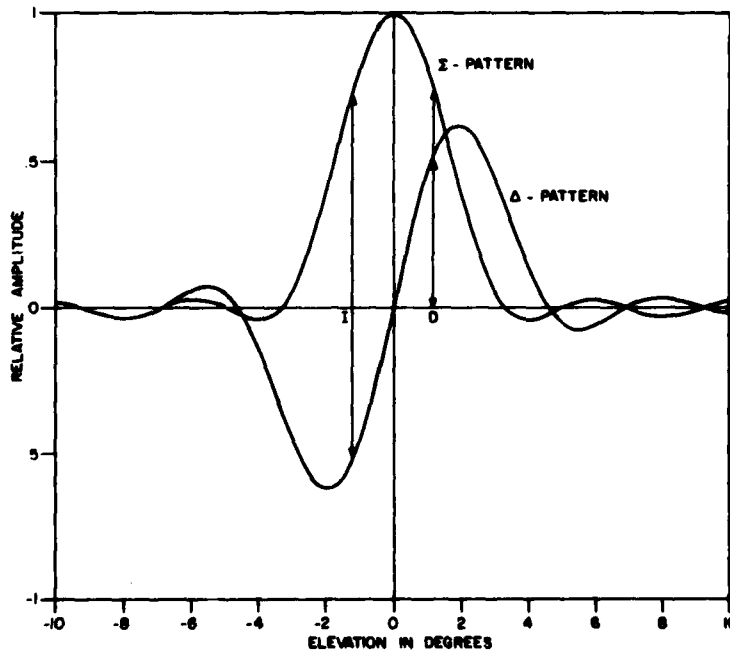
$$\varepsilon_M^Q = 0. \qquad\qquad (A.9)$$

Figure A.1. Typical Monopulse Sum (Σ) and Difference (Δ) Patterns